Detecting quantum gravitational effects in the early universe

Anzhong Wang

Physics Department, Baylor University, USA
&
Institute for Advanced Physics and Mathematics
Zhejiang University of Technology, China

Physics Department, Kobe University, Kobe, Japan

May 20, 2015

Table of Contents

In Collaboration with:

- Gerald Cleaver, Physics Depart., Baylor University
- Klaus Kirsten, Math Depart., Baylor University
- Qin Sheng, Math Depart., Baylor University
- Qiang Wu, Institute for Advanced Physics and Mathematics, Zhejiang University of Technology
- Tao Zhu, Institute for Advanced Physics and Mathematics, Zhejiang University of Technology & Physics Depart., Baylor University

Based on:

- "*Detecting quantum gravitational effects of loop quantum cosmology in the early universe*," arXiv:1503.06761.
- "*Power spectra and spectral indices of* k*-inflation: high-order corrections*," PRD90 (2014) 103517 [arXiv:1407.8011].
- "*Quantum effects on power spectra and spectral indices with higher-order corrections*," PRD90 (2014) 063503 [arXiv: 1405.5301].
- "*Inflationary cosmology with nonlinear dispersion relations*," PRD89 (2014) 043507 [arXiv:1308.5708].
- "*Constructing analytical solutions of linear perturbations of inflation with modified dispersion relations*," IJMPA29 (2014) 1450142 [arXiv:1308.1104].

Table of Contents

1.1 Why inflation?

(A. Guth, PRD23 (1981) 347)

- It solves the problems of standard big bang cosmology: flatness, horizon, cosmic relics, etc.
- It provides a causal mechanism for generations of adiabatic, Gaussian, and nearly scale-invariant primordial fluctuations, which leads to
  - the formation of large scale structure of the universe;
  - the Cosmic Microwave Background (CMB) anisotropies.
- Inflation is remarkably successful and its predictions are matched to observations with astonishing precision.[1]

[1] Planck Collaboration, arXiv:1502.02114.

1.2 Quantum Fluctuations During Inflation

(D. Baumann, arXiv:0907.5424)

- According to the inflation paradigm, the large-scale structure of our universe and CMB all originated from *quantum fluctuations produced during Inflation, which can be decomposed into:* scalar, vector and tensor.

- But, because of the expansion of the universe and particular nature of the fluctuations, vector perturbations did not grow, and observationally can be safely ignored.

1.2 Quantum Fluctuations During Inflation (Cont.)

- Scalar and tensor perturbations are described by mode functions $\mu_{\rm k}(\eta)$,

$$\mu_{\rm k}'' + \left(\omega_{\rm k}^2 - \frac{{\rm z}''}{\rm z}\right)\mu_{\rm k} = 0, \quad {\rm z} \equiv \begin{cases} \frac{{\rm a}\phi'}{\mathcal{H}}, & {\rm scalar} \\ {\rm a}, & {\rm tensor} \end{cases}$$

  - $\omega_{\rm k}^2$: energy of the mode, and in general relativity (GR) is given by,

$$\omega_{\rm k}^2 = {\rm k}^2$$

  - ${\rm k}$: comoving wavenumber
  - ϕ: the scalar field — the inflaton; and $\phi' \equiv {\rm d}\phi/{\rm d}\eta$
  - η: the conform time, ${\rm d}\eta \equiv {\rm dt}/{\rm a(t)}$
  - ${\rm a}(\eta)$: the expansion factor of the universe; and $\mathcal{H} \equiv {\rm a}'/{\rm a}$

1.2 Quantum Fluctuations During Inflation (Cont.)

- Power spectra, $\Delta_{\rm i}^2$, are defined as,

$$\Delta_{\rm i}^2 \equiv \frac{{\rm k}^3}{2\pi^2}\left|\frac{\mu_{\rm k}}{\rm z}\right|_{\rm i}^2, \ ({\rm i}={\rm S},{\rm T}).$$

- Spectral indexes are defined as

$$n_{\rm s} \equiv 1 + \frac{{\rm d}\,\ln\Delta_{\rm s}^2({\rm k})}{{\rm d}\,\ln{\rm k}}, \quad n_{\rm T} \equiv \frac{{\rm d}\,\ln\Delta_{\rm T}^2({\rm k})}{{\rm d}\,\ln{\rm k}}.$$

- The ratio r is defined as,

$$r \equiv \frac{\Delta_{\rm T}^2}{\Delta_{\rm S}^2}.$$

1.3 Precision Cosmological Mearsurments

- Since the first measurement of CMB in 1964 by Penzias and Wilson (PW), there have been a variety of experiments to measure its radiation anisotropies and polarization, such as WMAP, PLanck and BICEP2, with ever increasing precision.

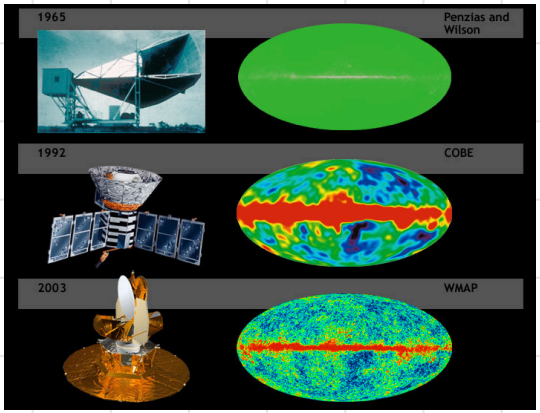

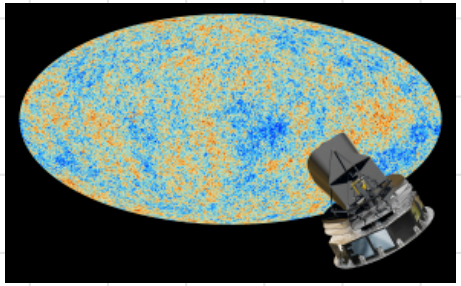

PW, COBE, WMAP　　Planck　　BICEP2

1.3 Precision Cosmological Mearsurments (cont.)

- In the coming decade, we anticipate that various new surveys will make even more accurate CMB measurements:
  - Balloon experiments: Balloon-borne Radiometers for Sky Polarisation Observations (BaR-SPoRT); The E and B Experiment (EBEX); ...
  - Ground experiments: Cosmology Large Angular Scale Surveyor (CLASS); Millimeter-Wave Bolometric Interferometer (MBI-B); Qubic; ...
  - Space experiments: Sky Polarization Observatory (SPOrt); ...

1.3 Precision Cosmological Mearsurments (cont.)

- In addition to CMB measurements, Large-scale structure surveys, measuring the galaxy power spectrum and the position of the baryon acoustic peak, have provided independently valuable information on the evolution of the universe.
- The first measurement of the kind started with the baryon acoustic oscillation (BAO) in the SDSS LRG and 2dF Galaxy surveys [2].

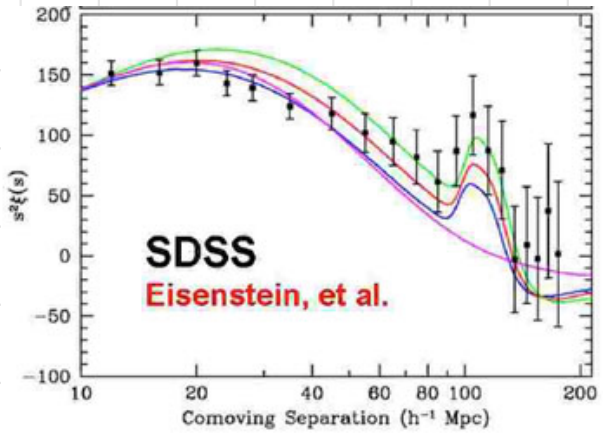

[2] D. J. Eisenstein, et al., ApJ 633 (2005) 560; S. Cole, et al., MNRAS362 (2005) 505.

1.3 Precision Cosmological Mearsurments (cont.)

- Since then, various large-scale structure surveys have been carried out [3], and provided sharp constraint on the budgets that made of the universe.

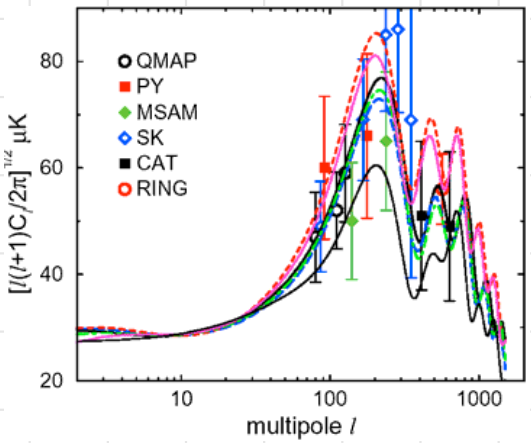

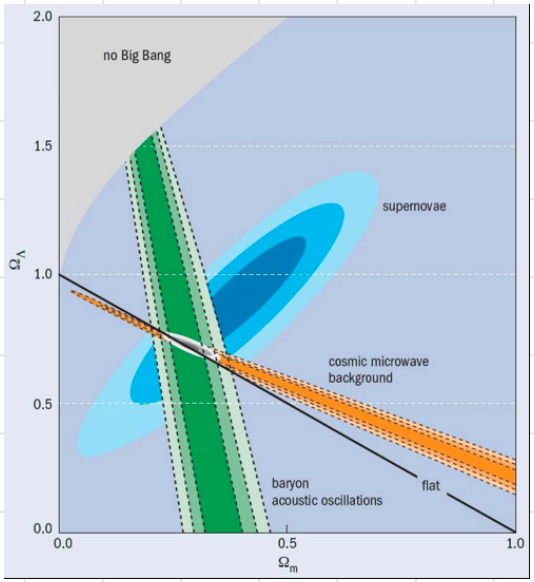

[3]Tegmark, M., et al. 2006, Phys. Rev. D, 74, 123507; Percival, W. J., Nichol, R. C., Eisenstein, D. J., et al. 2007, ApJ, 657, 51; Kazin, E. A., et al. 2010, ApJ, 710, 1444; Blake, C., Kazin, E., Beutler, F., et al. 2011, MNRAS, 418, 1707.

1.3 Precision Cosmological Mearsurments (cont.)

- Various new surveys will make even more accurate measurements of the galaxy power spectrum:
  - Ground-Based: the Prime Focus Spectrograph, Big BOSS, ...
  - Space-based: Euclid, WFIRST, ...
- Cosmology indeed enters its golden age: Precision Cosmology!

1.3 Precision Cosmological Mearsurments (cont.)

- In particular, the Stage IV experiments [4] will measure the physical variables

$$\sigma(\mathrm{n_s}, \mathrm{r}) = 10^{-3}$$

  - $\mathrm{n_s}$: the spectral index of scalar perturbations
  - r: the ratio between tensor and scalar perturbations

- With this level of uncertainty, the Stage IV experiments will make a clear detection ($> 5\sigma$) of tensor modes from any inflationary model with $\mathrm{r} \geq 0.01$.

---

[4] K. N. Abazajian et al., "Inflation physics from the cosmic microwave background and large scale structure", Astropart. Phys. 63, 55 (2015) [arXiv:1309.5381].

1.3 Precision Cosmological Measurments (cont.)

- Note that current measurements (Stage II) are from Planck 2015 [Planck Collaboration, arXiv:1502.02114],

$$\mathrm{n_s} = 0.968 \pm 0.006$$

$$\mathrm{r_{0.002}} < 0.11 \ (95 \ \% \ \mathrm{CL})$$

Table of Contents

2.1 Trans-Planckian Problem

(Brandenberger and Martin, CGQ30 (2013) 113001)

But, inflation is very sensitive to Planck-scale physics, and its origin has still remained elusive.

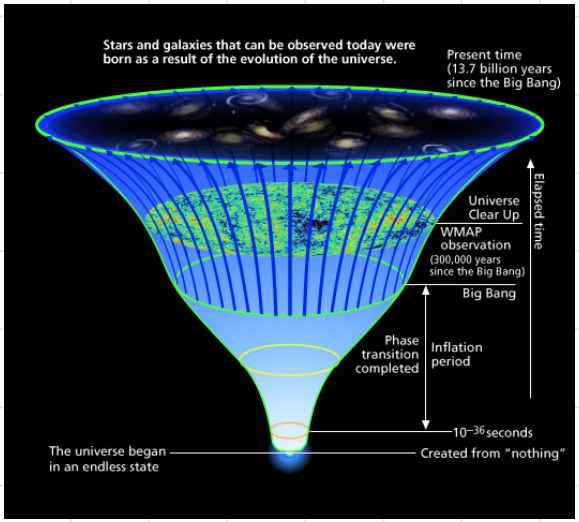

- In particular, during inflation the wavelengths, related to present observations, were exponentially stretched.
- To be consistent with observations, the inflationary period needs to be lasting long enough. If it is more than 70 e-folds, the wavelengths corresponding to present observations, should be smaller than the Planck length at the beginning of the inflation, and quantum gravitational effects become important
  — the trans-Planckian problem.

2.2 The η- problem:

- For a single inflaton field ϕ, its potential $V(\phi)$ must be very flat,

$$\epsilon_V \equiv M_{pl}^2 \left(\frac{V_{,\phi}}{V}\right)^2 \ll 1,$$

$$\eta_V \equiv \frac{M_{pl}^2}{2}\left(\frac{V_{,\phi\phi}}{V}\right) \ll 1,$$

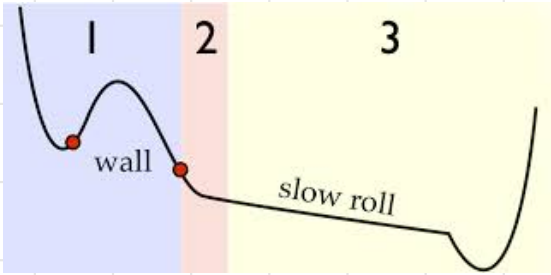

in order for the universe to expand large enough to solve the problems of big bang model, mentioned above.

2.2 The η- problem:

- In effective field theory (EFT), the cutoff energy scale Λ is defined by the lightest particle that is not included in the spectrum of the low-energy theory, and the effects of high energy scale physics above the energy Λ will change the coefficients of operators in the form,

$$\frac{\mathcal{O}_\delta}{\Lambda^{\delta-4}},$$

δ: the mass dimension of the operator

$\Lambda \simeq \mathrm{M_{pl}}$

2.2 The η- problem (Cont.):

- Then, in the absence of any specific symmetries to protect the inflation potential, dimension 4 and 6 operators will produce contributions to the potential of the forms,

$$\Delta \mathrm{V}(\phi) = \mathrm{c}_0 \frac{\langle \mathcal{O}_6 \rangle}{\mathrm{M}_{\mathrm{pl}}^2} + \mathrm{c}_1 \frac{\langle \mathcal{O}_4 \rangle}{\mathrm{M}_{\mathrm{pl}}^2} \phi^2,$$

$\mathrm{c}_0, \mathrm{c}_1$: dimensionless constants of order $\mathcal{O}(1)$. Then, for $\langle \mathcal{O}_4 \rangle \simeq \mathrm{V}$, we find that

$$\Delta \eta_{\mathrm{V}} \equiv \frac{\mathrm{M}_{\mathrm{pl}}^2}{2} \Delta \left(\frac{\mathrm{V}_{,\phi\phi}}{\mathrm{V}} \right) \simeq \mathrm{c}_1 \simeq \mathcal{O}(1),$$

which prevents a long-time exponential expansion — the η problem, which can be addressed so far only in string theory.

2.2 Planckian Excursion of Inflaton

(Lyth, PRL78 (1997) 1861)

- In the slow-roll approximations of a single scalar field, the change of the inflaton ϕ during inflation is given by,

$$\frac{\Delta\phi}{M_{pl}} \simeq \sqrt{\frac{r}{8}}\ \Delta N,$$

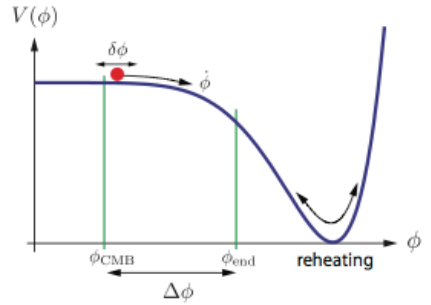

  - ΔN: the number of e-fold, corresponding to when the observed scales in the CMB leave the inflationary horizon

- If r does not change as a function of N, this directly leads to

$$\frac{\Delta\phi}{M_{pl}} \simeq \mathcal{O}(1)\sqrt{\frac{r}{0.01}}.$$

2.2 Planckian Excursion of Inflaton (Cont.)

- Then, the effective field theory of inflation with a potential $V(\phi)$, which consists of power expansion of operators suppressed by Planck scale,

$$V(\phi) = V^{\rm eff}(\phi) + \mathcal{O}\left[\left(\frac{\Delta\phi}{M_{\rm pl}}\right)^n\right],$$

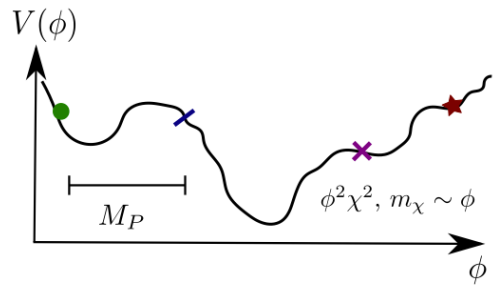

becomes questionable, and we need to take all the high-order corrections into account, unless additional symmetry is added, for example, a shift symmetry [5],

$$\phi \to \phi + \phi_0.$$

[5] L. McAllister, E. Silverstein, A. Westphal, T. Wrase, JHEP09(2014)123 [arXiv:1405.3652] and references therein.

2.3 Initial Conditions:

- Many inflationary scenarios only work if the fields are initially very homogeneous and/or start with precise initial positions and velocities. Any physical understanding of this "fine-tuning" requires a more complete formulation with ever-higher energies, such as string theory.
- ...

Therefore: Inflation is very sensitive to Planck-scale physics, and quantum gravitational effects in the early universe are important.

2.4 Experimental Tests for Quantum Gravity:

- On the other hand, quantization of gravity has been one of the main driving forces in physics in the past decades, and various approaches have been pursued, including String/M-Theory, loop quantum gravity, Horava-Lifshitz theory.

- However, it is fair to say that our understanding of them is still highly limited, and none of the aforementioned approaches is complete.

- One of the main reasons is the lack of experimental guides, due to the extreme weakness of gravitational fields.

2.4 Experimental Tests for Quantum Gravity (Cont.):

- This situation has been dramatically changed recently, with the arrival of the era of precision cosmology [6].
- One of our goals is to develop an ACCURATE and EFFECTIVE mathematical tool to study quantum gravitational effects in the early universe, whereby place these theories of quantum gravity directly under observational tests.
- Although it is very ambitious, I am going to argue that this becomes possible, with the great advance, happening recently in cosmological observations.

---

[6] C. Kiefer, and M. Kramer, Phys. Rev. Lett. 108, 021301 (2012); L.M. Krauss and F. Wilczek, Phys. Rev. D89, 047501 (2014); R.P. Woodard, arXiv:1407.4748.

2.4 Quantum Gravitational Effects

- **String/M-Theory:** As the most promising candidate for a UV-completion of the Standard Model that unifies gauge and gravitational interaction in a consistent quantum theory, String/M theory can provide possibilities for an explicit realization of the inflationary scenario.
- String/M theory usually leads to a non-trivial time-dependent speed of sound for primordial perturbations [7],

$$\omega_{\mathrm{k}}^2 = \mathrm{c}_{\mathrm{s}}^2(\eta)\mathrm{k}^2, \tag{1}$$

  - $\mathrm{c}_{\mathrm{s}}^2(\eta)$: the speed of sound, and could be very close to zero in the far UV regime.

[7] L. McAllister and E. Silverstein, Gen. Rel. Grav. 40, 565 (2007); C. P. Burgess, M. Cicoli, and F. Quevedo, arXiv: 1306.3512.

2.4 Quantum Gravitational Effects (Cont.)

- **Loop quantum cosmology (LQC):** Offers a natural framework to address the trans-Planckian issue and initial singularity.
- In particular, because effects of its underlying quantum geometry dominates at the Planck scale, leading to singularity resolution in a variety of cosmological models, where the initial singularity is replaced by the big bounce.
- There are mainly two kinds of quantum corrections to the cosmological background and perturbations[8]:
  (a) holonomy, and (b) inverse-volume

[8] M. Bojowald and G.M. Hossain, PRD78 (2008) 063547; M. Bojowald, G.M. Hossain, M. Kagan, and S. Shankaranarayanan, PRD79 (2009) 043505; 82, 109903 (E) (2010).

2.4 Quantum Gravitational Effects (Cont.)

- Due to the holonomy corrections, the dispersion relation in the mode functions is modified to

$$\omega_{\mathrm{k}}^2 = \left(1 - 2\frac{\rho(\eta)}{\rho_{\mathrm{c}}}\right)\mathrm{k}^2 \tag{2}$$

  - ρ_{c}: the energy density at which the big bounce happens.

- Due to the inverse-volume corrections, the dispersion relation in the mode functions is modified to

$$\omega_{\mathrm{k}}^2 = \mathrm{k}^2 \times \begin{cases} 1 + \left[\frac{\sigma\nu_0}{3}\left(\frac{\sigma}{6}+1\right) + \frac{\alpha_0}{2}\left(5-\frac{\sigma}{3}\right)\right]\delta_{\mathrm{PL}}(\eta), & \mathrm{scalar} \\ 1 + 2\alpha_0\delta_{\mathrm{PL}}, & \mathrm{tensor} \end{cases} \tag{3}$$

  - $\alpha_0,\ \nu_0,\ \sigma$: encode the specific features of the model
  - $\delta_{\mathrm{PL}}(\eta)$: time-dependent, given by $\delta_{\mathrm{PL}} = (\mathrm{a}_{\mathrm{PL}}/\mathrm{a})^{\sigma} < 1,$ with $\sigma > 0$.

2.4 Quantum Gravitational Effects (Cont.)

- To quantize gravity using quantum field theory, in 2009 Horava proposed a theory - Horava-Lifshitz (HL) gravity [9], which is power-counting renormalizable, and has attracted lot of attention since then.
- In this theory, the dispersion relation is modified to [AW and R. Maartens, PRD81 (2010) 024009; AW, PRD82 (2010) 124063],

$$\omega_k^2(\eta) = k^2 - b_1 \frac{k^4}{a^2 M_*^2} + b_2 \frac{k^6}{a^4 M_*^4} \tag{4}$$

  - M_*: the energy scale of the HL gravity
  - b_1, b_2: depend on the coupling constants of the HL theory and the type of perturbations, scalar or tensor.

[9] P. Horava, PRD79 (2009) 084008.

Table of Contents

3.1 Modified Equation of Mode Function

- Taking the quantum effects into account, either from string/M-Theory, or loop Quantum Cosmology, or HL gravity, or any of other theories, the equation of motion for the mode function $\mu_{\rm k}$ can be cast in the general form,

$$\frac{{\rm d}^2\mu_{\rm k}({\rm y})}{{\rm dy}^2} = \big[{\rm g}({\rm y}) + {\rm q}({\rm y})\big]\mu_{\rm k}({\rm y}), \tag{5}$$

$\rm g(y),\ q(y)$: functions of $\rm y[\equiv -k\eta]$, to be determined by minimizing the errors.

- For example, in the HL gravity, we have

$$\rm g(y) + q(y) \quad = \quad \frac{\nu^2 - 1/4}{y^2} - 1 + b_1\epsilon_*^2 y^2 - b_2\epsilon_*^4 y^4,$$

with $\epsilon_* \equiv {\rm H/M_*}, {\rm z''/z} \equiv (\nu^2(\eta) - 1/4)/\eta^2$.

3.1 Modified Equation of μ_k (Cont.)

- It is should be noted that the evolution of the mode function with the non-linear dispersion relation given by Eq.(6) had been already studied since 2001 [10], as toy models to mimic quantum gravitational effects.
- This is well before 2009 when Horava first proposed his theory, in which this non-linear dispersion relation is naturally produced as the result of power-counting renormalizability of the theory.

---

[10] J. Martin and R.H. Brandenberger, PRD63 (2001) 123501; D65 (2002) 103514; D68 (2003) 063513; J.C. Niemeyer and R. Parentani, D64 (2001) 101301 (R); L. Bergstorm and U.H. Danielsson, JHEP12 (2002) 038; J. Martin and C. Ringeval, PRD69 (2004) 083515; R. Easther, W. H. Kinney, and H. Peiris, JCAP 05 (2005) 009; M.G. Jackson and K. Schalm, PRL 108 (2012) 111301.

3.1 Modified Equation of $\mu_{\rm k}$ (Cont.)

- However, in all these studies, the Brandenberger-Martin (BM) approximation [PRD65 (2002) 103514] was used,

$$\mu_{\rm k}(\eta)=\begin{cases}\dfrac{1}{\sqrt{2\omega_{\rm k}(\eta)}}{\rm e}^{-{\rm i}\int_{\eta_{\rm i}}^{\eta}\omega_{\rm k}(\eta'){\rm d}\eta'}, & \text{when } \eta<\eta_1,\\ {\rm C}_{+}{\rm a}(\eta)+{\rm C}_{-}{\rm a}(\eta)\int_{\eta_1}^{\eta}\dfrac{{\rm d}\eta'}{{\rm a}^2(\eta')}, & \text{when } \eta_1<\eta<\eta_2,\\ \dfrac{\alpha_{\rm k}{\rm e}^{-{\rm i}\int_{\eta_2}^{\eta}\omega_{\rm k}(\eta'){\rm d}\eta'}+\beta_{\rm k}{\rm e}^{{\rm i}\int_{\eta_2}^{\eta}\omega_{\rm k}(\eta'){\rm d}\eta'}}{\sqrt{2\omega_{\rm k}(\eta)}}, & \text{when } \eta_2<\eta<\eta_3,\\ {\rm D}_{+}{\rm a}(\eta)+{\rm D}_{-}{\rm a}(\eta)\int_{\eta_3}^{\eta}\dfrac{{\rm d}\eta'}{{\rm a}^2(\eta')}, & \text{when } \eta>\eta_3.\end{cases}$$

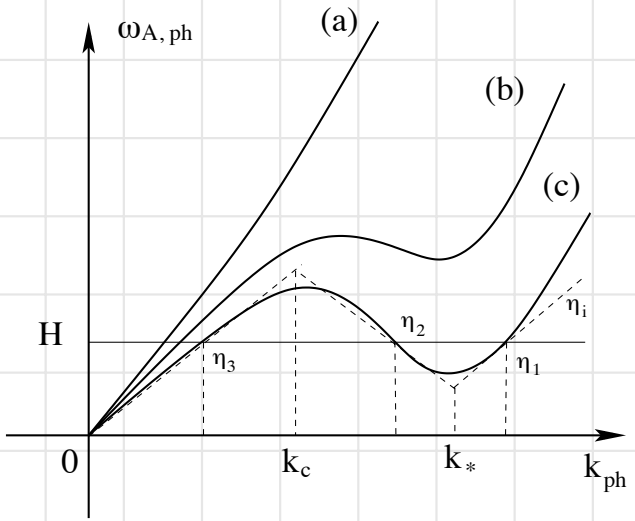

3.1 Modified Equation of $\mu_{\rm k}$ (Cont.)

- Its validity in various physics situations has been questioned [S.E. Joras and G. Marozzi, PRD79 (2009) 023514]:
  - The approximations break down at the matching points (η_1, η_2, and η_3), and thus the errors becomes large.
  - Numerical calculations showed it is only valid when the comoving wavenumer $\mathrm{k} \gg \mathrm{aH}$.
  - The error bounds for the solutions are not known, so they are not under any control.

3.1 Modified Equation of μ_{k} (Cont.)

- In the following, I am going to present *the uniform asymptotic approximation method,* developed recently by us, which has the following advantages:
  - The error bounds are given explicitly. By properly choosing the functions $\mathrm{g(y)}$ and $\mathrm{q(y)}$, we can minimize the errors, so that analytical solutions with high accuracy can be constructed to high orders.
  - Up to the third-order approximations in terms of the parameter λ, introduced in the method, the errors are

$$\delta \lesssim 0.15\%$$

3.2 Liouville Transformations

- The strategy is to use the well-established Liouville transformations to introduce
  - a new variable ξ, instead of y,
  - a new function U, instead of μ_{k},

$$\mathrm{y} \to \xi,$$

$$\mu_{\mathrm{k}}(\mathrm{y}) \to \mathrm{U}(\xi),$$

- so that the resulted equation can be solved:
  - analytically order by order in terms of $\epsilon \equiv 1/\lambda \ll 1$
  - the corresponding error bounds are well under control at each step, so the errors can be minimized

3.2 Liouville Transformations (Cont.)

- The Liouville Transformations are

$$\begin{aligned} \mathrm{U}(\xi) &= \chi^{1/4}\mu_{\mathrm{k}}(\mathrm{y}), \qquad \chi \equiv \xi'^2 = \frac{|\mathrm{g}(\mathrm{y})|}{\mathrm{f}^{(1)}(\xi)^2}, \\ \mathrm{f}(\xi) &= \int^{\mathrm{y}} \sqrt{|\mathrm{g}(\mathrm{y})|}\mathrm{dy}, \qquad \mathrm{f}^{(1)}(\xi) = \frac{\mathrm{df}(\xi)}{\mathrm{d}\xi}, \end{aligned} \tag{6}$$

- χ must be regular and not vanish in the intervals of interest
- $\mathrm{g}(\mathrm{y})$ & $\mathrm{q}(\mathrm{y})$ are properly chosen to minimize the errors
- $\mathrm{f}^{(1)}(\xi)$ must be chosen so that it has zeros and singularities of the same type as that of $\mathrm{g}(\mathrm{y})$

3.2 Liouville Transformations (Cont.)

- The equation of motion for the mode function reduces to,

$$\frac{\mathrm{d}^2\mathrm{U}(\xi)}{\mathrm{d}\xi^2} = \left[\pm \mathrm{f}^{(1)}(\xi)^2 + \psi(\xi)\right]\mathrm{U}(\xi), \tag{7}$$

with

$$\psi(\xi) = \frac{\mathrm{q}(\mathrm{y})}{\chi} - \chi^{-3/4}\frac{\mathrm{d}^2(\chi^{-1/4})}{\mathrm{dy}^2}, \tag{8}$$

in the above "$+$" for $\mathrm{g}(\mathrm{y}) > 0$, and "$-$" for $\mathrm{g}(\mathrm{y}) < 0$.

- Neglecting $\psi(\xi)$ we obtain solutions to the first-order approximation
- Choosing properly $\mathrm{f}^{(1)}(\xi)$ in order for the equation to be:
  (a) solved analytically, and
  (b) minimizing the error bounds.

3.2 Liouville Transformations (Cont.)

- To solve the differential equation for the new function $\mathrm{U}(\xi)$ analytically, we divide the task into three steps:
  - Solve it near some singular points,

$$\mathrm{g}(\mathrm{y}) + \mathrm{q}(\mathrm{y}) = \pm\infty,$$

    often called poles.
  - Solve it near the turning points,

$$\mathrm{g}(\mathrm{y}) = 0.$$

  - Then, matching all the solutions together with the initial conditions, which are normally taken as the Bunch-Davies (adiabatic) vacuum.

3.3 Solutions near poles

- To illustrate our method, in the following we shall restrict ourselves to the case,

$$\begin{aligned} g(y) + q(y) &\equiv \left(\frac{z''}{z} - \omega_k^2 \right) k^{-2} \\ &= \frac{\nu^2 - 1/4}{y^2} - 1 + b_1 \epsilon_*^2 y^2 - b_2 \epsilon_*^4 y^4 \end{aligned}$$

although our method can be used for any given dispersion relation ω_k^2 and background z''/z.

- Eq.(9) has two poles (singularities), $y = 0, \infty$, and three turning points (roots of g(y)= 0).

3.3 Solutions near poles (Cont.)

- The functions $\mathrm{g(y)}$ and $\mathrm{q(y)}$ are well-defined near the two possible poles, $\mathrm{y} = 0^+,\ +\infty$. Thus, we choose

$$\mathrm{f}^{(1)}(\xi)^2 = 1, \qquad \xi = \int^{\mathrm{y}} \sqrt{|\mathrm{g(y)}|}\mathrm{dy},$$

so that

$$\frac{\mathrm{d}^2\mathrm{U}(\xi)}{\mathrm{d}\xi^2} = \Big[\pm 1 + \psi(\xi)\Big]\mathrm{U}(\xi),$$

here "$+$" for 0^+, and "$-$" for $+\infty$.

- By neglecting $\psi(\xi)$ as the first-order approximations, the solutions of the above equation can be determined analytically.

3.3 Solutions near poles (Cont.)

Near the pole $\mathrm{y} = 0^+$, the solutions are given by

$$\mu_{\mathrm{k}}^{+}(\mathrm{y}) = \frac{\mathrm{c}_+}{\mathrm{g(y)}^{1/4}} \mathrm{e}^{\int^{\mathrm{y}} \sqrt{\mathrm{g(y)}}\mathrm{dy}} (1 + \epsilon_1^+) + \frac{\mathrm{d}_+}{\mathrm{g(y)}^{1/4}} \mathrm{e}^{-\int^{\mathrm{y}} \sqrt{\mathrm{g(y)}}\mathrm{dy}} (1 + \epsilon_2^+),$$

$\epsilon_1^+,\ \epsilon_2^+$: represent the errors of the approximations,

$$\epsilon_1^+ = \frac{1}{2} \int_0^{\xi} \left(1 - \mathrm{e}^{2(\mathrm{v}-\xi)}\right) \psi(\mathrm{v}) \left(1 + \epsilon_1^+\right) \mathrm{dv},$$

$\xi \in (0, \mathrm{a}_1),\ \mathrm{v} \in (0, \xi],\ \mathrm{y} \in (0^+, \hat{\mathrm{a}}_1)$;

$\mathrm{a}_1,\ \hat{\mathrm{a}}_1$: the upper bounds of the variables $\xi,\ \mathrm{y}$

$\xi(0^+) = 0,\ \xi(\hat{\mathrm{a}}_1) = \mathrm{a}_1.$

3.3 Solutions near poles (Cont.)

Similar expression is for ϵ_2^+. Then, the error bounds are

$$|\epsilon_1^+|, \quad \frac{|\mathrm{d}\epsilon_1^+/\mathrm{dy}|}{2|\mathrm{g}|^{1/2}} \leq \exp\left(\frac{1}{2}\mathscr{V}_{0,\mathrm{y}}(\mathrm{F})\right) - 1,$$

$$|\epsilon_2^+|, \frac{|\mathrm{d}\epsilon_2^+/\mathrm{dy}|}{2|\mathrm{g}|^{1/2}} \leq \exp\left(\frac{1}{2}\mathscr{V}_{\mathrm{y},\hat{\mathrm{a}}_1}(\mathrm{F})\right) - 1,$$

where the error control function $\mathrm{F}(\mathrm{y})$ and $\mathscr{V}_{\mathrm{a,b}}(\mathrm{F})$ are defined as

$$\mathrm{F}(\mathrm{y}) = \int \left[\frac{1}{|\mathrm{g}|^{1/4}}\frac{\mathrm{d}^2}{\mathrm{dy}^2}\left(\frac{1}{|\mathrm{g}|^{1/4}}\right) - \frac{\mathrm{q}}{|\mathrm{g}|^{1/2}}\right]\mathrm{dy},$$

$$\mathscr{V}_{\mathrm{a,b}}(\mathrm{F}) \equiv \int_{\mathrm{a}}^{\mathrm{b}} \left|\frac{\mathrm{dF}(\mathrm{y})}{\mathrm{dy}}\right| \mathrm{dy}$$

3.3 Solutions near poles (Cont.)

Near the pole $y = +\infty$, the solutions are given by

$$\mu_k^-(y) = \frac{c_-}{|g(y)|^{1/4}} e^{\int^y \sqrt{|g(y)|}dy}(1+\epsilon_1^-) + \frac{d_-}{|g(y)|^{1/4}} e^{-\int^y \sqrt{|g(y)|}dy}(1+\epsilon_2^-),$$

ϵ_1^-, ϵ_2^-: represent the errors of the approximations, and have similar expressions as those for ϵ_1^+, ϵ_2^+.

3.4 Solutions near turning points

- Error Control Function and Choice of $g(y)$ and $q(y)$:
  The convergence of the error control function $F(y)$ requires that one must choose [PRD89 (2014) 043507],

$$
\begin{aligned}
g(y) &= \frac{\nu^2}{y^2} - 1 + b_1 \epsilon_*^2 y^2 - b_2 \epsilon_*^4 y^4, \\
q(y) &= -\frac{1}{4y^2}.
\end{aligned}
$$

- Then, $g(y)$, usually has three roots, ($y_0,\ y_1,\ y_2$), where
  - we assume $0 < y_0 < \mathrm{Re}(y_1) \le \mathrm{Re}(y_2)$
  - y_0 is always real and positive
  - when $y_1,\ y_2$ real, we assume $y_1 \le y_2$
  - When $y_1,\ y_2$ are complex, we have $y_1 = y_2^*$.

3.4 Solutions near turning points (Cont.)

The turning points are defined as the roots of

$$g(y) = \frac{\nu^2}{y^2} - 1 + b_1 \epsilon_*^2 y^2 - b_2 \epsilon_*^4 y^4 = 0.$$

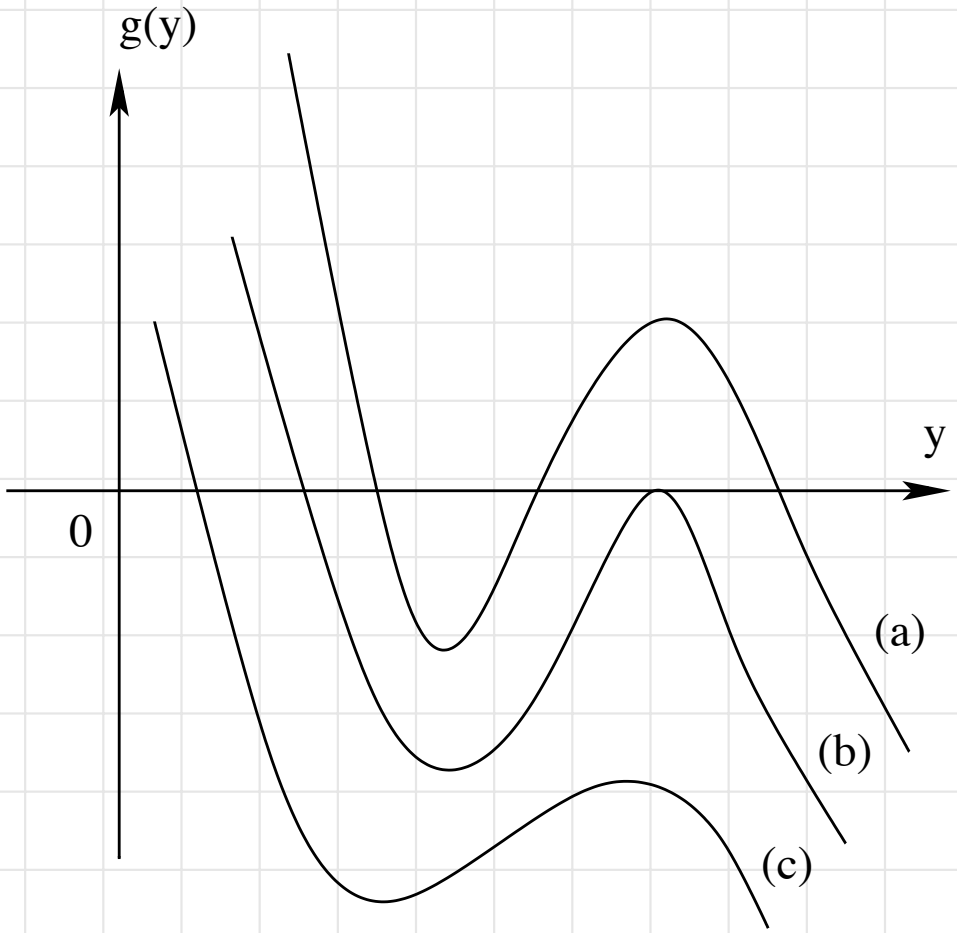

3.4 Solutions near turning points (Cont.)

- Approximate solution around $\mathrm{y} = \mathrm{y}_0$: Since y_0 is a single zero of $\mathrm{g}(\mathrm{y}) = 0$, we can choose $\mathrm{f}^{(1)}(\xi)^2 = \pm\xi$, so that

$$\frac{\mathrm{d}^2\mathrm{U}(\xi)}{\mathrm{d}\xi^2} = \Big(\xi + \psi(\xi)\Big)\mathrm{U}(\xi),$$

which has the approximate solution,

$$\begin{aligned}\mu_{\mathrm{k}}(\mathrm{y}) \;=\; & \alpha_0 \left(\frac{\xi}{\mathrm{g}(\mathrm{y})}\right)^{1/4} \Big(\mathrm{Ai}(\xi) + \epsilon_3\Big) \\ & + \beta_0 \left(\frac{\xi}{\mathrm{g}(\mathrm{y})}\right)^{1/4} \Big(\mathrm{Bi}(\xi) + \epsilon_4\Big),\end{aligned}$$

$\mathrm{Ai}(\xi)$, $\mathrm{Bi}(\xi)$: the Airy functions

ϵ_3, ϵ_4: the errors of the approximations

3.4 Solutions near turning points (Cont.)

- The error ϵ_3 is given by

$$\epsilon_3(\xi) = \int_{\xi}^{\mathrm{a}_3} \mathcal{K}(\xi, \mathrm{v})|\mathrm{v}|^{-1/2}\psi(\mathrm{v})\Big(\mathsf{Ai}(\mathrm{v}) + \epsilon_3\Big),$$

a_3: the upper bound of ξ; $\hat{\mathrm{a}}_3$: the upper bound of y, with $\xi(\hat{\mathrm{a}}_3) = \mathrm{a}_3$.

- A similar expression for ϵ_4. Then, the up bounds are

$$\frac{|\epsilon_3|}{\mathrm{M}(\xi)}, \frac{|\partial\epsilon_3/\partial\xi|}{\mathrm{N}(\xi)} \leq \frac{\mathrm{E}^{-1}(\xi)}{\lambda}\Big\{\exp\Big(\lambda\mathscr{V}_{\xi,\mathrm{a}_3}(\mathrm{H})\Big) - 1\Big\},$$
$$\frac{|\epsilon_4|}{\mathrm{M}(\xi)}, \frac{|\partial\epsilon_4/\partial\xi|}{\mathrm{N}(\xi)} \leq \frac{\mathrm{E}(\xi)}{\lambda}\Big\{\exp\Big(\lambda\mathscr{V}_{\mathrm{a}_4,\xi}(\mathrm{H})\Big) - 1\Big\},$$

but now with the error control function $\mathrm{H}(\mathrm{y})$ defined as $\mathrm{H}(\xi) = \int_{\xi}^{\mathrm{a}_3} |\mathrm{v}|^{-1/2}\psi(\mathrm{v})\mathrm{dv}$.

3.4 Solutions near turning points (Cont.)

- Approximate solutions around $\mathrm{y} = (\mathrm{y}_1,\ \mathrm{y}_2)$: Near these turning points, we choose

$$\mathrm{f}^{(1)}(\xi)^2 = |\xi^2 - \xi_0^2|, \quad \xi_0^2 = \pm\frac{2}{\pi}\left|\int_{\mathrm{y}_1}^{\mathrm{y}_2}\sqrt{|\mathrm{g}(\mathrm{y})|}\mathrm{dy}\right|,$$

  - " $\pm$ " correspond $\mathrm{y}_{1,2}$ are real and complex, respectively
  - when $\mathrm{y}_{1,2}$ are both real, ξ_0 is positive
  - when $\mathrm{y}_{1,2}$ are both complex, ξ_0 is purely imaginary
  - when $\mathrm{y}_1 = \mathrm{y}_2$, they degenerate to a double turning point, and $\xi_0 = 0$

3.4 Solutions near turning points (Cont.)

- Then, the solutions around y_1 and y_2 are given by

$$\begin{aligned}\mu_{\mathrm{k}}(\mathrm{y}) &= \alpha_1 \left(\frac{\xi^2-\xi_0^2}{-\mathrm{g}(\mathrm{y})}\right)^{1/4} \left[\mathrm{W}\left(\frac{1}{2}\xi_0^2, \sqrt{2}\xi\right) + \epsilon_5\right] \\ &\quad + \beta_1 \left(\frac{\xi^2-\xi_0^2}{-\mathrm{g}(\mathrm{y})}\right)^{1/4} \left[\mathrm{W}\left(\frac{1}{2}\xi_0^2, -\sqrt{2}\xi\right) + \epsilon_6\right],\end{aligned}$$

$\epsilon_5,\ \epsilon_6$: the errors of the approximations

$\mathrm{W}\left(\frac{1}{2}\xi_0^2, \pm\sqrt{2}\xi\right)$: the cylindrical functions

3.4 Solutions near turning points (Cont.)

- The error ϵ_5 is given by

$$\epsilon_5(\xi) = \int_{\xi}^{\mathrm{a}_5} \mathcal{K}(\xi, \mathrm{v}) \frac{\psi(\mathrm{v})}{\mathrm{v}} \left\{ \mathrm{W}\left(\frac{1}{2}\xi_0^2, \sqrt{2}\mathrm{v}\right) + \epsilon_5 \right\} \mathrm{dv},$$

$$\mathcal{K}(\xi, \mathrm{v}) = \mathrm{v}\left\{ \mathrm{W}\left(\frac{1}{2}\xi_0^2, \sqrt{2}\xi\right) \mathrm{W}\left(\frac{1}{2}\xi_0^2, -\sqrt{2}\mathrm{v}\right) - \mathrm{W}\left(\frac{1}{2}\xi_0^2, \sqrt{2}\mathrm{v}\right) \mathrm{W}\left(\frac{1}{2}\xi_0^2, -\sqrt{2}\xi\right) \right\}.$$

a_5: is the upper bound of ξ.

- A similar expression is for ϵ_6.

3.4 Solutions near turning points (Cont.)

- The up error bounds are

$$\frac{|\epsilon_5|}{\mathrm{M}\left(\frac{1}{2}\xi_0^2, \sqrt{2}\xi\right)}, \frac{|\partial\epsilon_5/\partial\xi|}{\sqrt{2}\mathrm{N}\left(\frac{1}{2}\xi_0^2, \sqrt{2}\xi\right)} \leq \frac{\kappa}{\lambda \mathrm{E}\left(\frac{1}{2}\xi_0^2, \sqrt{2}\xi\right)} \left\{ \exp\left(\lambda \mathscr{V}_{\xi,\mathrm{a}_5}(\mathrm{H})\right) - 1 \right\},$$

$$\frac{|\epsilon_6|}{\mathrm{M}\left(\frac{1}{2}\xi_0^2, \sqrt{2}\xi\right)}, \frac{|\partial\epsilon_6/\partial\xi|}{\sqrt{2}\mathrm{N}\left(\frac{1}{2}\xi_0^2, \sqrt{2}\xi\right)} \leq \frac{\kappa \mathrm{E}\left(\frac{1}{2}\xi_0^2, \sqrt{2}\xi\right)}{\lambda} \left\{ \exp\left(\lambda \mathscr{V}_{0,\xi}(\mathrm{I})\right) - 1 \right\}.$$

3.5 Matching to the Initial solution

- We assume the universe was initially at the adiabatic (Bunch-Davies) vacuum,

$$\begin{aligned}\lim_{y\to+\infty}\mu_k(y) &= \frac{1}{\sqrt{2\omega}}e^{-i\int\omega d\eta}\\ &\simeq \sqrt{\frac{k}{2}}\frac{1}{(-g)^{1/4}}\exp\left(-i\int_{y_i}^{y}\sqrt{-g}dy\right).\end{aligned}$$

- Since the equation of the mode function is second-order, we need one more condition to completely fix the free parameters in the solutions. We choose the second one as the Wronskian condition

$$\mu_k(y)\mu_k^*(y)' - \mu_k^*(y)\mu_k(y)' = i.$$

3.5 Matching to the Initial solution (Cont.)

- We found four sets of solutions:
  - LG solution near the pole $y = \infty$ with (c_-, d_-)
  - Cylindrical function solution near the two turning points $y_{1,2}$ with (α_1, β_1)
  - Airy function solution near the turning point y_0 with (α_0, β_0)
  - LG solution near the pole $y = 0$ with (c_+, d_+)

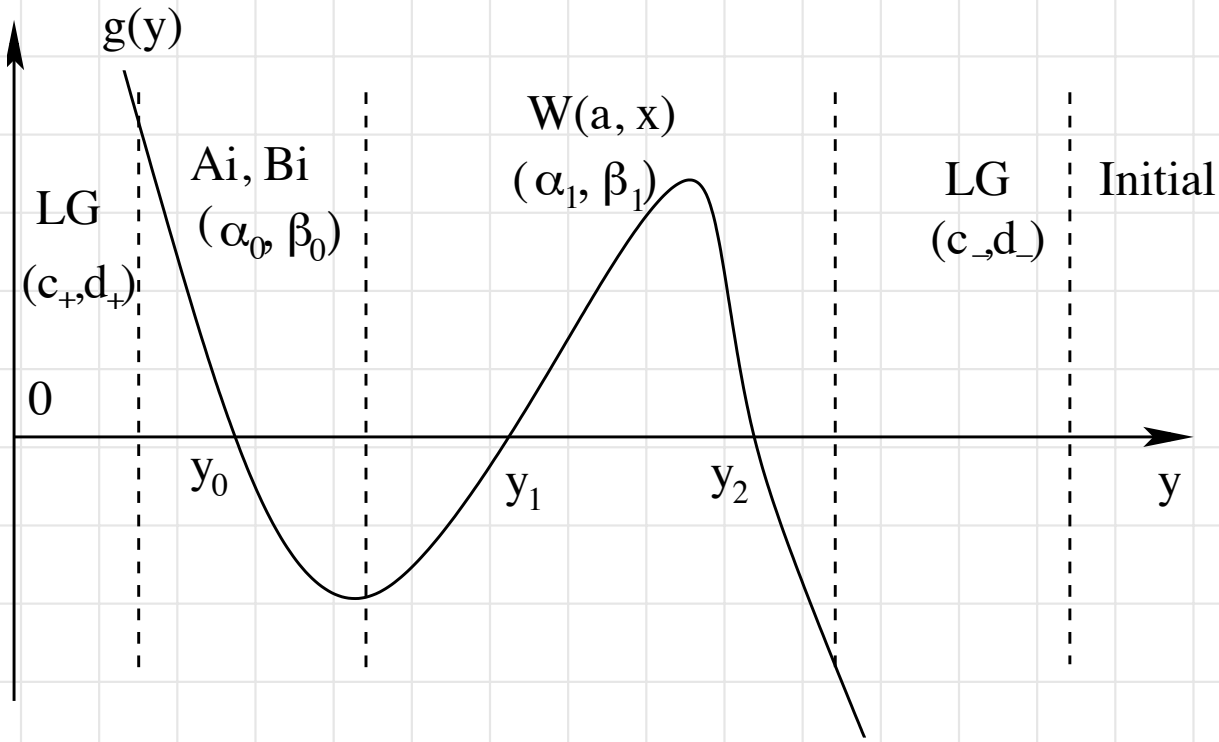

3.5 Matching to the Initial solution (Cont.)

- Using the initial conditions to the LG solution near the pole $\mathrm{y} = \infty$, we find that

$$\mathrm{C}_- = 0, \quad \mathrm{d}_- = \sqrt{\frac{1}{2\mathrm{k}}}.$$

- Matching the LG solution with the cylindrical function solutions at $\mathrm{y} \gg \mathrm{y}_2$ we find that

$$\begin{aligned} \alpha_1 &= 2^{-3/4}\mathrm{k}^{-1/2}\,\mathrm{j}^{-1/2}(\xi_0), \\ \beta_1 &= -\mathrm{i}2^{-3/4}\mathrm{k}^{-1/2}\,\mathrm{j}^{1/2}(\xi_0), \end{aligned}$$

with $\mathrm{j}(\xi_0) \equiv \sqrt{1 + \mathrm{e}^{\pi\xi_0^2}} - \mathrm{e}^{\pi\xi_0^2/2}$.

3.5 Matching to the Initial solution (Cont.)

- Matching the cylindrical function solution with the Airy function one in their common region $\mathrm{y} \in (\mathrm{y}_0, \mathrm{y}_1)$, we find

$$\alpha_0 = \sqrt{\frac{\pi}{2\mathrm{k}}}\left[\mathrm{j}^{-1}(\xi_0)\sin\mathfrak{B} - \mathrm{i}\,\mathrm{j}(\xi_0)\cos\mathfrak{B}\right],$$

$$\beta_0 = \sqrt{\frac{\pi}{2\mathrm{k}}}\left[\mathrm{j}^{-1}(\xi_0)\cos\mathfrak{B} + \mathrm{i}\,\mathrm{j}(\xi_0)\sin\mathfrak{B}\right],$$

where

$$\mathfrak{B} \equiv \int_{\mathrm{y}_0}^{\mathrm{y}_1} \sqrt{-\mathrm{g}}\mathrm{d}\mathrm{y} + \phi(\xi_0^2/2),$$

$$\phi(\mathrm{x}) \equiv \frac{\mathrm{x}}{2} - \frac{\mathrm{x}}{4}\ln\mathrm{x}^2 + \frac{1}{2}\mathsf{ph}\Gamma\left(\frac{1}{2} + \mathrm{i}\mathrm{x}\right).$$

3.5 Matching to the Initial solution (Cont.)

- Finally, matching the LG solution near the pole $\mathrm{y} = 0$ with the Airy function one in their common region $\mathrm{y} \in (0, \mathrm{y}_0)$, we find

$$\begin{aligned} \mathrm{d}_+ &= \frac{\alpha_0}{2\sqrt{\pi}} \exp\left(-\int_{0+}^{\mathrm{y}_0} \sqrt{\mathrm{g}}\mathrm{dy}\right), \\ \mathrm{c}_+ &= \frac{\beta_0}{\sqrt{\pi}} \exp\left(\int_{0+}^{\mathrm{y}_0} \sqrt{\mathrm{g}}\mathrm{dy}\right). \end{aligned}$$

3.6 Comparing with numerical (exact) solutions

- When $y_{1,2}$ are real and $y_1 \neq y_2$:

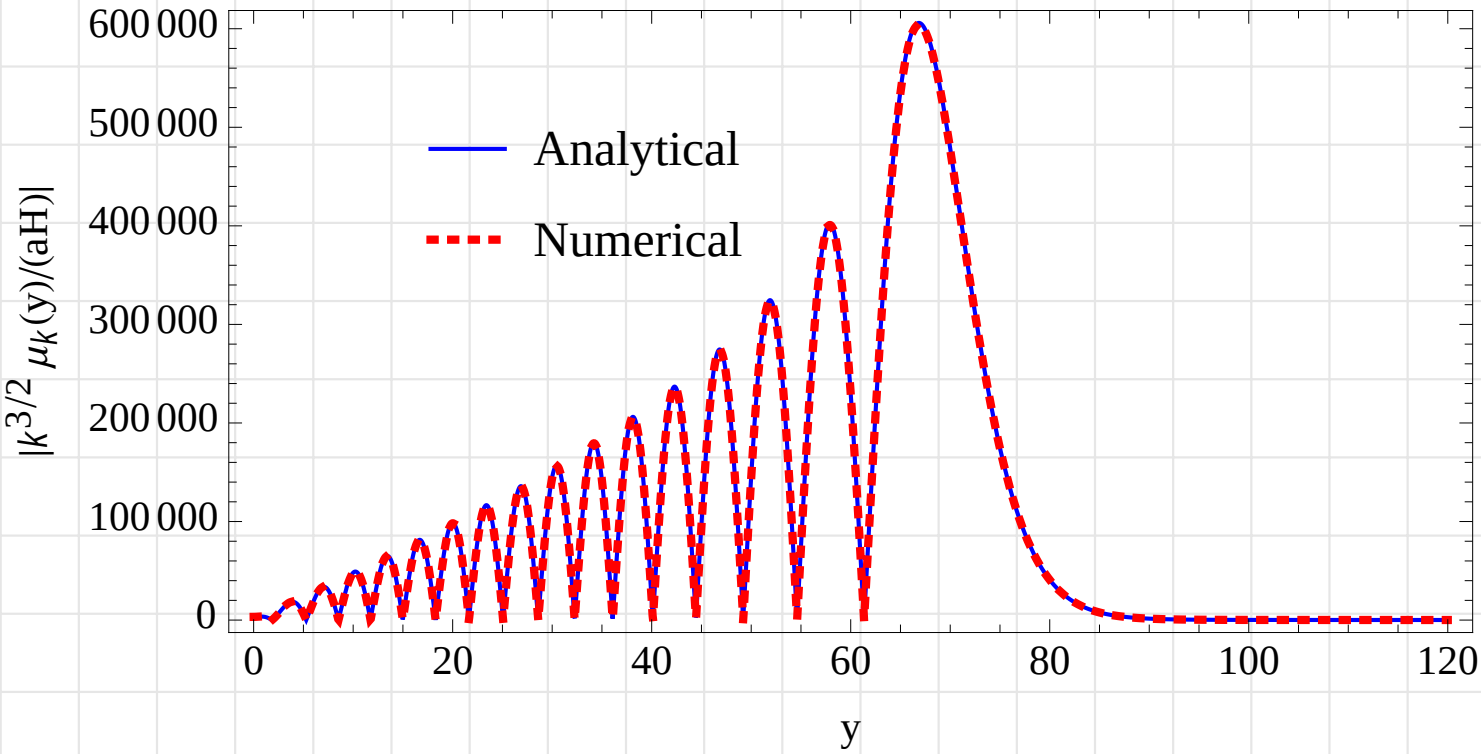

Figure : The numerical (exact) (red dotted curves) and analytical (blue solid curves) solutions with $b_1 = 3$, $b_2 = 2$, $\nu = 3/2$, and $\epsilon_* = 0.01$.

3.6 Comparing with numerical (exact) solutions (Cont.)

- When $y_{1,2}$ are real and $y_1 = y_2$:

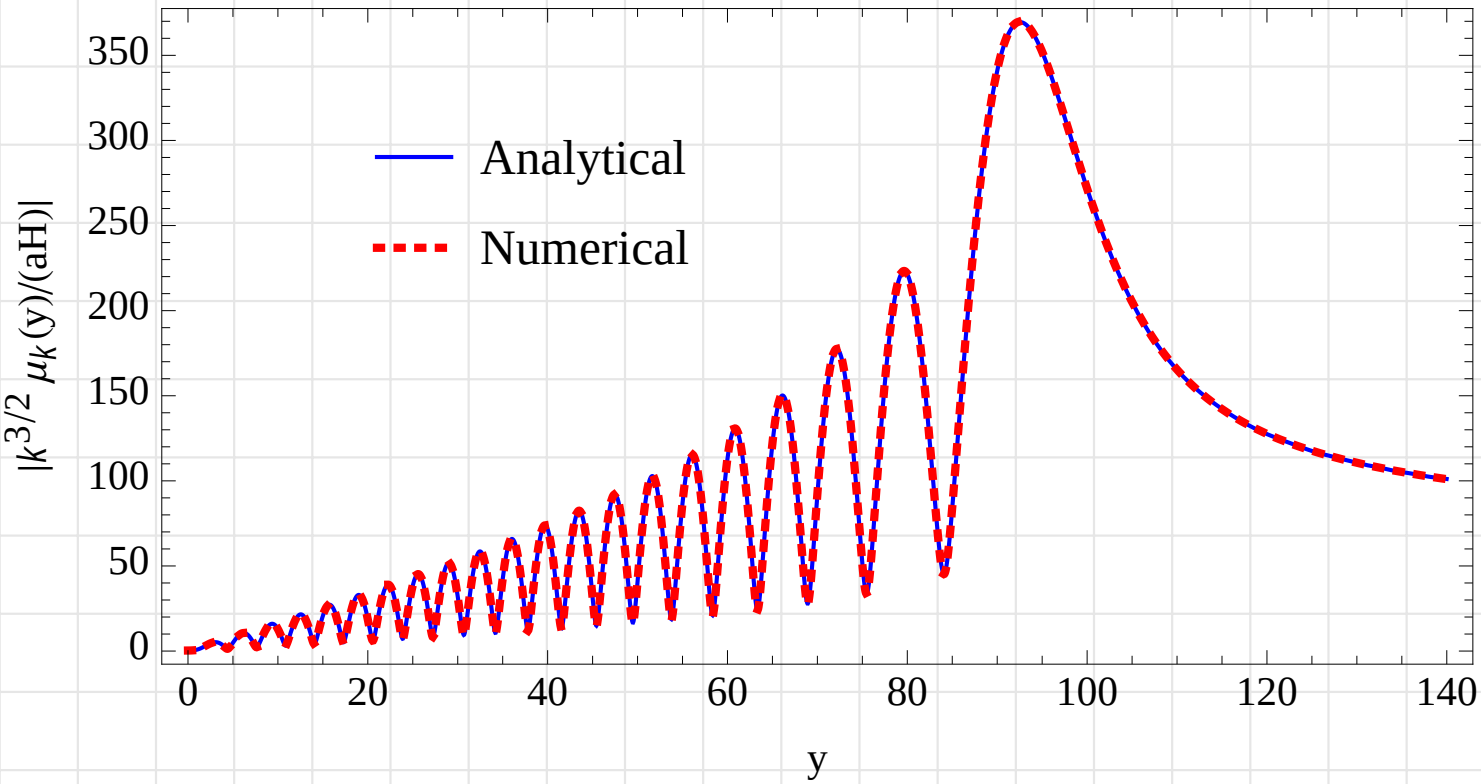

Figure : The numerical (exact) (red dotted curves) and analytical (blue solid curves) solutions with $b_1 = 2$, $b_2 = 1.00023$, $\nu = 3/2$, and $\epsilon_* = 0.01$.

3.6 Comparing with numerical (exact) solutions (Cont.)

- When $y_{1,2}$ are complex:

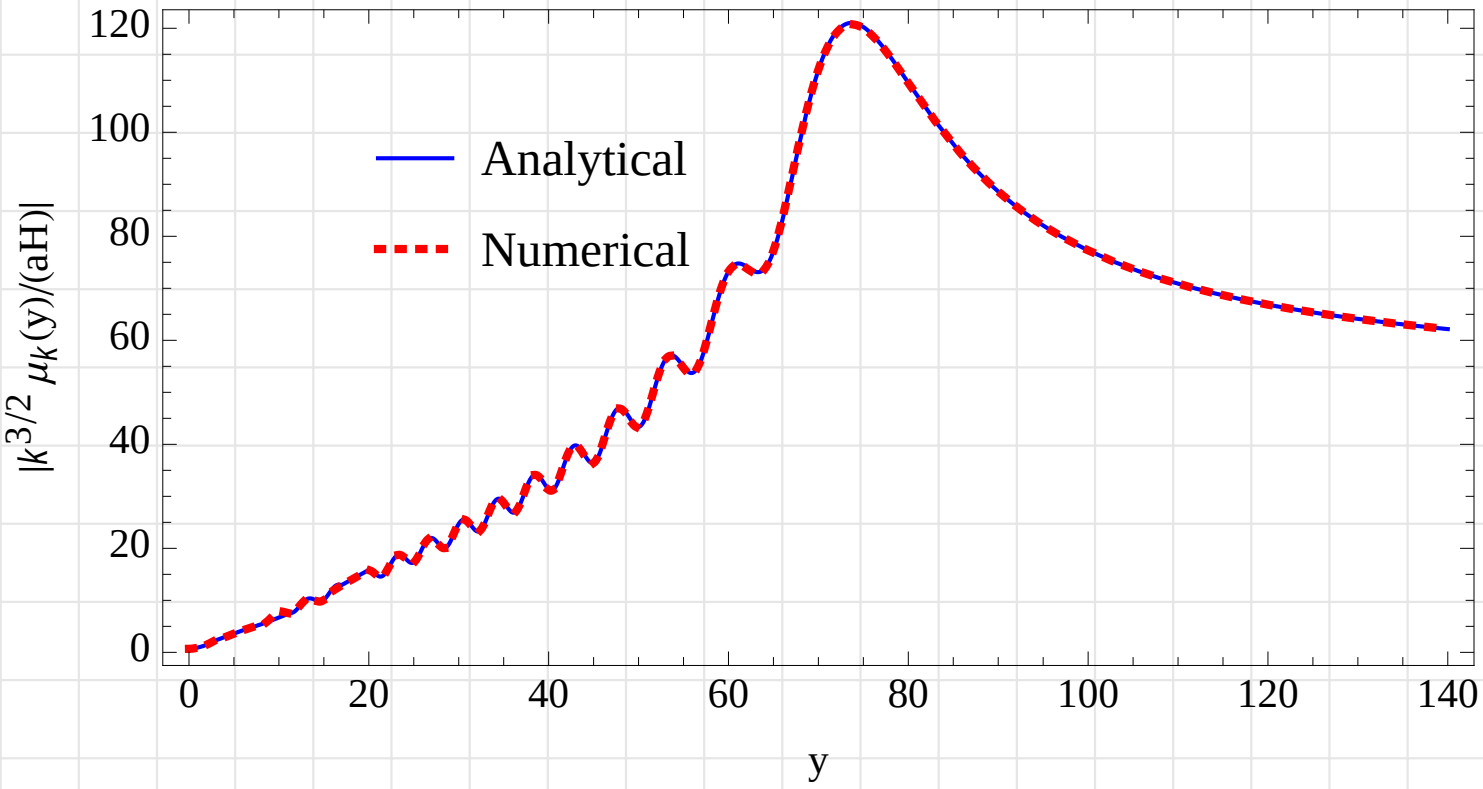

Figure : The numerical (exact) (red dotted curves) and analytical (blue solid curves) solutions with $b_1 = 3.5$, $b_2 = 3.2$, $\nu = 3/2$, and $\epsilon_* = 0.01$.

3.7 High-order Corrections

- To generalize the above to high-order approximation is challenging, mainly because of the matching. So, in the following we consider the case where $\mathrm{g}(\mathrm{y}) = 0$ has only one real root, y_0.
- Then, we can choose

$$\mathrm{f}^{(1)}(\xi) = \pm\xi,$$

$\xi = \xi(\mathrm{y})$: a monotone decreasing function

"+": corresponds to $\mathrm{g}(\mathrm{y}) \geq 0$

"-": corresponds to $\mathrm{g}(\mathrm{y}) \leq 0$.

3.7 High-order Corrections (Cont.)

- Then, the mode function $\mathrm{U}(\xi)$ is given by

$$
\begin{aligned}
\mathrm{U}(\xi) \;=\; \alpha_0 \Bigg[& \mathrm{Ai}(\lambda^{2/3}\xi) \sum_{\mathrm{s}=0}^{\mathrm{n}} \frac{\mathrm{A_s}(\xi)}{\lambda^{2\mathrm{s}}} \\
& + \frac{\mathrm{Ai}'(\lambda^{2/3}\xi)}{\lambda^{4/3}} \sum_{\mathrm{s}=0}^{\mathrm{n}-1} \frac{\mathrm{B_s}(\xi)}{\lambda^{2\mathrm{s}}} + \epsilon_3^{(2\mathrm{n}+1)} \Bigg] \\
+\beta_0 \Bigg[& \mathrm{Bi}(\lambda^{2/3}\xi) \sum_{\mathrm{s}=0}^{\mathrm{n}} \frac{\mathrm{A_s}(\xi)}{\lambda^{2\mathrm{s}}} \\
& + \frac{\mathrm{Bi}'(\lambda^{2/3}\xi)}{\lambda^{4/3}} \sum_{\mathrm{s}=0}^{\mathrm{n}-1} \frac{\mathrm{B_s}(\xi)}{\lambda^{2\mathrm{s}}} + \epsilon_4^{(2\mathrm{n}+1)} \Bigg], \qquad (9)
\end{aligned}
$$

where α_0 and β_0 are two integration constants.

3.7 High-order Corrections (Cont.)

- The coefficients A_s and B_s are given by

$$A_0(\xi) = 1,$$

$$B_s = \frac{\pm 1}{2(\pm\xi)^{1/2}} \int_0^{\xi} \{\psi(v)A_s(v) - A_s''(v)\} \frac{dv}{(\pm v)^{1/2}},$$

$$A_{s+1}(\xi) = -\frac{1}{2}B_s'(\xi) + \frac{1}{2}\int \psi(v)B_s(v)dv, (s = 0, 1, 2, ...) \quad (10)$$

where "+" corresponds to $\xi \geq 0$, and "-" to $\xi \leq 0$.

3.7 High-order Corrections (Cont.)

- The error bounds of $\epsilon_3^{(2n+1)}$ and $\epsilon_4^{(2n+1)}$ are given by,

$$\frac{\epsilon_3^{(2n+1)}}{M(\lambda^{2/3}\xi)}, \quad \frac{\partial\epsilon_3^{(2n+1)}/\partial\xi}{\lambda^{2/3}N(\lambda^{2/3}\xi)}$$

$$\leq 2E^{-1}(\lambda^{2/3}\xi)\exp\left[\frac{2\kappa_0\mathcal{V}_{\alpha,\xi}(|\xi^{1/2}|B_0)}{\lambda}\right]$$

$$\times\frac{\mathcal{V}_{\alpha,\xi}(|\xi^{1/2}|B_n)}{\lambda^{2n+1}},$$

$$\frac{\epsilon_4^{(2n+1)}}{M(\lambda^{2/3}\xi)}, \quad \frac{\partial\epsilon_4^{(2n+1)}/\partial\xi}{\lambda^{2/3}N(\lambda^{2/3}\xi)}$$

$$\leq 2E(\lambda^{2/3}\xi)\exp\left[\frac{2\kappa_0\mathcal{V}_{\xi,\beta}(|\xi^{1/2}|B_0)}{\lambda}\right]$$

$$\times\frac{\mathcal{V}_{\xi,\beta}(|\xi^{1/2}|B_n)}{\lambda^{2n+1}}.$$

3.7 High-order Corrections (Cont.)

- To determine α_0 and β_0, we assume the same initial conditions as in the firs-order approximations, that is, the universe initially was in the Bunch-Davies vacuum, and μ_{k} satisfies the Wronskian condition,

$$\lim_{\mathrm{y}\to+\infty}\mu_{\mathrm{k}}(\mathrm{y})=\frac{1}{\sqrt{2\omega_{\mathrm{k}}}}\mathrm{e}^{-\mathrm{i}\int\omega_{\mathrm{k}}\mathrm{d}\eta},$$
$$\mu_{\mathrm{k}}(\mathrm{y})\mu_{\mathrm{k}}^{*}(\mathrm{y})'-\mu_{\mathrm{k}}^{*}(\mathrm{y})\mu_{\mathrm{k}}(\mathrm{y})'=\mathrm{i}.$$

- After tedious calculations, we surprisingly find a very simple result,

$$\alpha_0=\sqrt{\frac{\pi}{2\mathrm{k}}},\quad \beta_0=\mathrm{i}\sqrt{\frac{\pi}{2\mathrm{k}}}.$$

3.8 Power spectra and spectral indexes with High-order Corrections

- To the third-order approximations, the power spectrum is given by

$$\begin{aligned}\Delta^2(\mathrm{k}) &\equiv \frac{\mathrm{k}^3}{2\pi^2}\left|\frac{\mu_{\mathrm{k}}(\mathrm{y})}{\mathrm{z}}\right|^2_{\mathrm{y}\to 0^+} \\ &= \frac{\mathrm{k}^2}{4\pi^2}\frac{-\mathrm{k}\eta}{\mathrm{z}^2(\eta)\nu^2(\eta)}\exp\left(2\int_{\mathrm{y}}^{\nu_0}\sqrt{\hat{\mathrm{g}}(\hat{\mathrm{y}})}\mathrm{d}\hat{\mathrm{y}}\right) \\ &\quad\times\left[1+\frac{\mathrm{H}(+\infty)}{\lambda}+\frac{\mathrm{H}^2(+\infty)}{2\lambda^2}+\mathcal{O}(1/\lambda^3)\right].\end{aligned} \tag{11}$$

3.8 Power spectra and spectral indexes with High-order Corrections (Cont.)

- To the third-order approximations, the spectral index is given by

$$\mathrm{n}-1 \equiv \frac{\mathrm{d}\ln\Delta^2(\mathrm{k})}{\mathrm{d}\ln\mathrm{k}} = 3 + 2\int_{\mathrm{y}}^{\nu_0}\frac{\mathrm{d}\hat{\mathrm{y}}}{\sqrt{\hat{\mathrm{g}}(\hat{\mathrm{y}})}} + \frac{1}{\lambda}\frac{\mathrm{dH}(+\infty)}{\mathrm{d}\ln\mathrm{k}} + \mathcal{O}\left(\frac{1}{\lambda^3}\right). \quad (12)$$

- Note that the order of the approximations is referred to $1/\lambda$, and we have not impose the slow-roll conditions, normally denoted by ϵ_{n}, adopted in inflation.
- ϵ_{n} and λ^{-1} are two set of independent parameters. So, our method can be equally applied to non-slow-roll cases.

3.9 Applications to Special Cases

- High-order power spectra and spectral indices have been calculated so far up to the second-order of the slow-roll parameters only in two cases:

  (a) GR ($\omega_{\rm k}^2 = {\rm k}^2$), first by using the Green function method and later confirmed by the improved WKB method[11],

  (b) k-inflation ($\omega_{\rm k}^2 = {\rm c}_{\rm s}^2(\eta){\rm k}^2$), by using the uniform approximation method but to the firs-order of $(1/\lambda)$[12].

---

[11] J.-O. Gong and E.D. Stewart, PLB510 (2001) 1; S.M. Leach, A, Liddle, J. Martin and D. Schwarz, PRD66 (2002) 023515; J.-O. Gong, CQG21 (2004) 5555; R. Casadio, et al, PRD71 (2005) 043517; PLB625 (2005) 1.

[12] J. Martin, C. Ringeval and V. Vennin, JCAP06 (2013) 021.

3.9 Applications to Special Cases (Cont.)

- Applying our method to GR up to the second-order in terms of the slow-roll parameters ϵ_n and the third-order in terms of λ, we find that the exact (numerical) solutions are extremely well approximated by our analytical solutions [PRD90 (2014) 063503, arXiv:1405.5301].

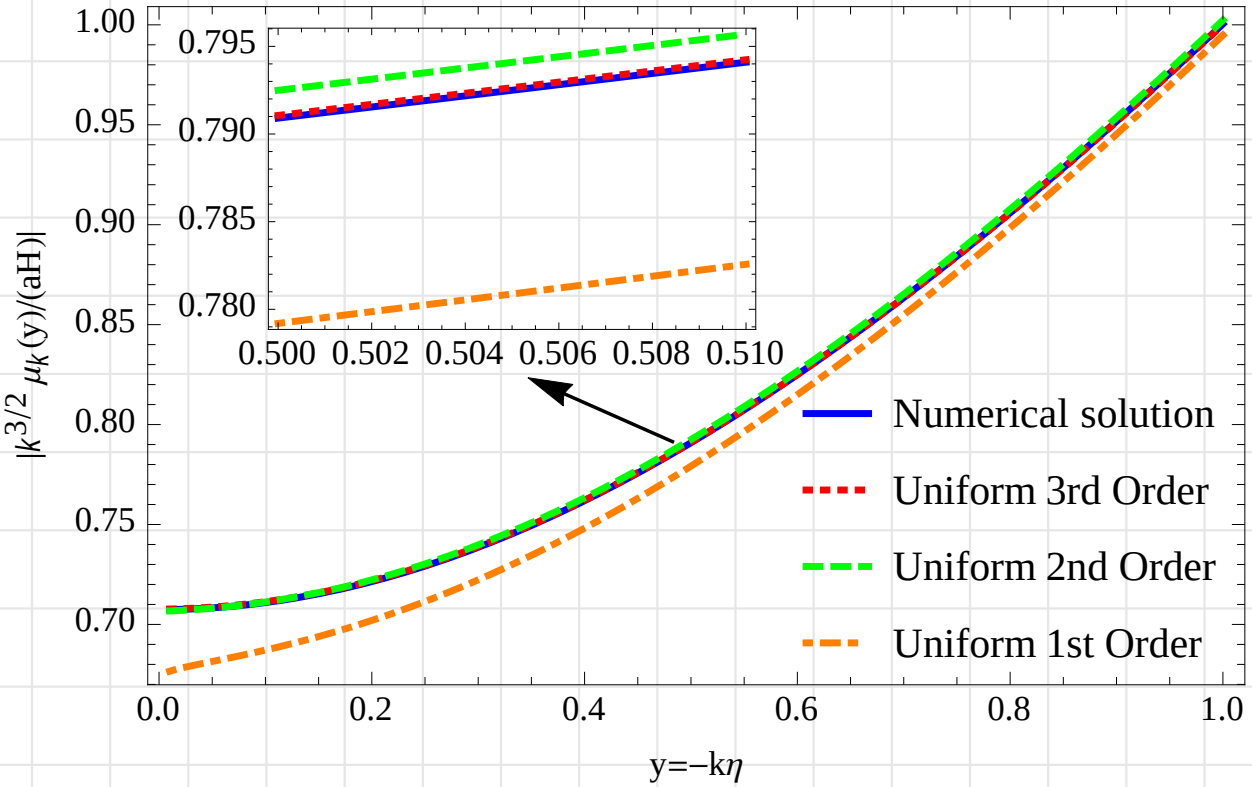

3.9 Applications to Special Cases (Cont.)

- The resulted power spectra and spectral indexes of both scalar and tensor perturbations are consistent with the ones obtained by the Green function and improved WKB methods[13], within the allowed errors [PRD90 (2014) 063503, arXiv:1405.5301].
- Applying our method to k-inflation, we obtained the power spectra, spectral indexes and runnings of both scalar and tensor perturbations with the highest accuracy existing in the literature so far [PRD90 (2014) 103517, arXiv:1407.8011].

---

[13] J.-O. Gong and E.D. Stewart, PLB510 (2001) 1; S.M. Leach, A, Liddle, J. Martin and D. Schwarz, PRD66 (2002) 023515; J.-O. Gong, CQG21 (2004) 5555; R. Casadio, et al, PRD71 (2005) 043517; PLB625 (2005) 1.

Table of Contents

4. Detecting Quantum Gravitational Effects in the Early Universe

- With the arrival of the era of the precision cosmology, it would be extremely important and interesting to see if any of these quantum gravitational effects in the early universe are within the range of the current and forthcoming experiments.
- In the following, we shall show that this is indeed possible. To be more specific, we concentrate ourselves on the inverse-volume corrections from LQC [14], for which the dispersion relations are,

---

[14] M. Bojowald and G. Calcagni, JCAP 03 (2011) 032; M. Bojowald, G. Calcagni, and S. Tsujikawa, Phys. Rev. Lett. 107, 211302 (2011); JCAP 11 (2011) 046.

4. Detecting Quantum Gravitational Effects in the Early Universe (Cont.)

$$\omega_{\rm k}^2 = {\rm k}^2 \times \begin{cases} 1 + \left[\frac{\sigma\nu_0}{3}\left(\frac{\sigma}{6}+1\right) + \frac{\alpha_0}{2}\left(5-\frac{\sigma}{3}\right)\right]\delta_{\rm PL}(\eta), & {\rm scalar} \\ 1 + 2\alpha_0\delta_{\rm PL}, & {\rm tensor} \end{cases}$$

- $\alpha_0,\ \nu_0,\ \sigma$: encode the specific features of the model, with

$$0 < \sigma \leq 6,$$

- $\delta_{\rm PL}(\eta)$: time-dependent,

$$\delta_{\rm PL} = \left(\frac{{\rm a_{PL}}}{\rm a}\right)^{\sigma} < 1,$$

${\rm a_{PL}}$: a constant.

4. Detecting Quantum Gravitational Effects in the Early Universe (Cont.)

Then, we find that,

$$
\begin{aligned}
\mathrm{n_s} &\simeq 1 - 2\epsilon_{\star 1} - \epsilon_{\star 2} - 2\epsilon_{\star 1}^2 - (3 + 2\mathrm{D_n})\,\epsilon_{\star 1}\epsilon_{\star 2} - \mathrm{D_n}\epsilon_{\star 2}\epsilon_{\star 3} \\
&\quad + \epsilon_{\mathrm{pI}}\left(\tfrac{3}{2}\mathrm{H}_\star\right)^{\sigma}\left(\mathcal{K}_{-1}^{\star(\mathrm{s})}\epsilon_{\star 1}^{-1} + \mathcal{K}_{0}^{\star(\mathrm{s})} + \mathcal{K}_{1}^{\star(\mathrm{s})}\epsilon_{\star 2}\epsilon_{\star 1}^{-1}\right), \\
\mathrm{r} &\simeq 16\epsilon_{\star 1}\left[1 + \mathrm{D_p}\epsilon_{\star 2} - \epsilon_{\mathrm{pI}}\left(\tfrac{3}{2}\mathrm{H}_\star\right)^{\sigma}\mathcal{Q}_{-1}^{\star(\mathrm{s})}\epsilon_{\star 1}^{-1}\right], \qquad (13)
\end{aligned}
$$

$\epsilon_1 \equiv -\dot{\mathrm{H}}/\mathrm{H}^2,\ \epsilon_{\mathrm{n}+1} \equiv \dot{\epsilon}_{\mathrm{n}}/(\mathrm{H}\epsilon_{\mathrm{n}}),\ \epsilon_{\mathrm{pI}} \equiv (\mathrm{a_{pI}}/\mathrm{k})^{\sigma}$,

$\mathrm{D_p} \equiv 67/181 - \ln 3,\ \mathrm{D_n} \equiv 10/27 - \ln 3$,

$\mathrm{f}_\star$: denoting its evaluation at horizon crossing,

$\mathrm{a}(\eta_\star)\mathrm{H}(\eta_\star) = \mathrm{s}(\eta_\star)\mathrm{k}$,

$\mathcal{K}_{-1}^{\star(\mathrm{s})},\ \mathcal{Q}_{-1}^{\star(\mathrm{s})}$: the leading terms, given in the following Table

4. Detecting Quantum Gravitational Effects in the Early Universe (Cont.)

Table : Values of Coefficients $\mathcal{Q}_{-1}^{\star(\mathrm{s})}$ & $\mathcal{K}_{-1}^{\star(\mathrm{s})}$

σ	1	2	3	4	5	6
$\mathcal{Q}_{-1}^{\star(\mathrm{s})}$	$\frac{\pi}{6}\alpha_0$	$\frac{2}{3}\alpha_0$	0	$\frac{-1616}{1629}\alpha_0$	$\frac{475}{2896}\pi\alpha_0$	$\frac{10512}{905}\alpha_0$
$\mathcal{K}_{-1}^{\star(\mathrm{s})}$	$-\frac{\pi}{6}\alpha_0$	$-\frac{4}{3}\alpha_0$	0	$\frac{320\alpha_0}{81}$	$-\frac{125}{144}\pi\alpha_0$	$-\frac{352}{5}\alpha_0$

When $\sigma = 3$, $\mathcal{Q}_{-1}^{\star(\mathrm{s})}$ and $\mathcal{K}_{-1}^{\star(\mathrm{s})}$ vanish, one has to consider contributions from $\mathcal{Q}_{0}^{\star(\mathrm{s})}$ and $\mathcal{K}_{0}^{\star(\mathrm{s})}$,

$$\mathcal{Q}_{0}^{\star(\mathrm{s})} = \frac{513\pi}{11584}\nu_0, \quad \mathcal{K}_{0}^{\star(\mathrm{s})} = -\frac{9\pi}{64}\nu_0.$$

4. Detecting Quantum Gravitational Effects in the Early Universe (Cont.)

The precision measurement of $(n_s,\ r)$ provides a promising detection of the quantum gravitational effects. In particular, future experiments, such as EUCLID, PRISM, and LiteBIRD [15], should be able to measure $(n_s,\ r)$ with errors down to 10^{-3},

$$\sigma(n_s) \simeq \sigma(r) \simeq 10^{-3}.$$

---

[15] L. Amendola et al. (Euclid Theory Working Group Collaboration), Living Rev. Relativity 16, 6 (2013); P. Andre et al. (PRISM Collaboration), arXiv:1306.2259; T. Matsumura et al., arXiv: 1311.2847.

4. Detecting Quantum Gravitational Effects in the Early Universe (Cont.)

Then, for $\mathrm{V}(\phi) = \lambda_{\mathrm{p}}\phi^{\mathrm{p}}$, we find that

$$\begin{aligned}\Gamma &\equiv (\mathrm{n_s} - 1) + \frac{\mathrm{p}+2}{8\mathrm{p}}\mathrm{r} + \gamma_1(\mathrm{n_s}-1)^2 \\ &= \mathcal{F}(\sigma)\frac{\delta(\mathrm{k}_\star)}{\epsilon_{\mathrm{V}}},\end{aligned} \tag{14}$$

where $\delta(\mathrm{k}) \equiv \alpha_0\delta_{\mathrm{PL}}(\mathrm{k})$,

$$\begin{aligned}\mathcal{F}(\sigma) &\sim \mathcal{O}(1), \quad \epsilon_{\mathrm{V}} \equiv \mathrm{M_{pl}^2 V_\phi^2/(2V^2)}, \\ \gamma_1 &= [3\mathrm{p}^2 + (18 - 12\mathrm{D_p} + 12\mathrm{D_n})\mathrm{p} + 24\mathrm{D_p} \\ &\quad -24\mathrm{D_n} - 4]/[6(\mathrm{p}+1)^2].\end{aligned}$$

$\mathcal{F}(\sigma)\frac{\delta(\mathrm{k}_\star)}{\epsilon_{\mathrm{V}}}$: the quantum gravitational effects from LQC.

4. Detecting Quantum Gravitational Effects in the Early Universe (Cont.)

Since $\sigma\left(\mathrm{n_s}\right) \simeq \sigma\left(\mathrm{r}\right) \simeq 10^{-3}$, we have

$$\sigma\left(\Gamma\right) \simeq 10^{-3}.$$

Therefore, if

$$\mathcal{F}(\sigma)\frac{\delta(\mathrm{k}_\star)}{\epsilon_{\mathrm{V}}} \gtrsim \mathcal{O}\left(10^{-3}\right),$$

the quantum gravitational effects from LQC is within the range of detection!

4. Detecting Quantum Gravitational Effects in the Early Universe (Cont.)

- Using our Cosmological Monte Carlo (CosmoMC) code[16] with the Planck, BAO, and Supernova Legacy Survey data[17], we first carry out our CMB likelihood analysis.
- In particular, we assume the flat cold dark matter model with effective number of neutrinos $N_{eff} = 3.046$ and fix the total neutrino mass $\Sigma m_{\nu} = 0.06 eV$.

---

[16] Y.-G. Gong, Q. Wu, and A. Wang, Astrophys. J. 681, 27-39 (2008); http://cosmologist.info/cosmomc

[17] P. A. R. Ade (Planck Collaboration), Astron. Astrophys. 571 (2014) A16; L. Anderson et al., Mon. Not. R. Astron. Soc. 427, 3435 (2013); A. Conley, J. Guy, M. Sullivan, N. Regnault, P. Astier, C. Balland, S. Basa and R. G. Carlberg et al., Astrophys. J. Suppl. 192, 1 (2011).

4. Detecting Quantum Gravitational Effects in the Early Universe (Cont.)

- We vary the seven parameters:
  (i) baryon density parameter, $\Omega_{\rm b}{\rm h}^2$
  (ii) dark matter density parameter, $\Omega_{\rm c}{\rm h}^2$
  (iii) the ratio of the sound horiozn to the angular diameter, θ
  (iv) the reionization optical depth, τ
  (v) $\delta({\rm k}_0)/\epsilon_{\rm V}$
  (vi) $\epsilon_{\rm V}$
  (vii) $\Delta^2_{\rm s}({\rm k}_0)$
- We take the pivot wave number ${\rm k}_0 = 0.05$ Mpc^{-1}, used in Planck, to constrain $\delta({\rm k}_0)$ and $\epsilon_{\rm V}$.

4. Detecting Quantum Gravitational Effects in the Early Universe (Cont.)

- The following figures show the constraints:

$$\delta(\mathrm{k}_0) \lesssim 6.8 \times 10^{-5}, \qquad \sigma = 1,$$
$$\delta(\mathrm{k}_0) \lesssim 1.9 \times 10^{-8}, \qquad \sigma = 2,$$

at 1σ (68% CL) level.

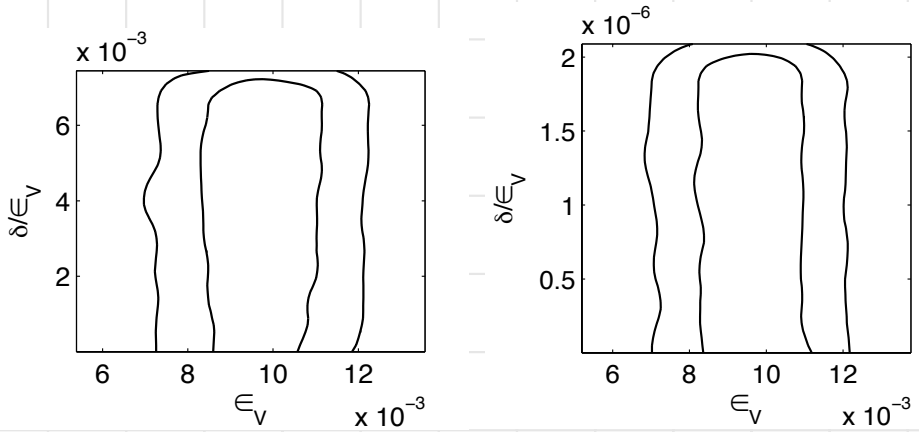

4. Detecting Quantum Gravitational Effects in the Early Universe (Cont.)

- The upper bound for $\delta(\mathrm{k}_0)$ decreases dramatically as σ increases.
- However, despite the tight constraints on $\delta(\mathrm{k}_0)$, because of the $\epsilon_{\mathrm{V}}^{-1}$ enhancement in Eq.(14), such effects can be well within the range of the detection of the current and forthcoming cosmological experiments[18] for

$$\sigma \lesssim 1,$$

which is favorable even theoretically[19].

[18] K. N. Abazajian et al., "Inflation physics from the cosmic microwave background and large scale structure", Astropart. Phys. 63, 55 (2015) [arXiv:1309.5381].

[19] M. Bojowald and G. Calcagni, JCAP 03 (2011) 032.

4. Detecting Quantum Gravitational Effects in the Early Universe (Cont.)

- It is remarkable to note that, for any given σ, the best fitting value of ϵ_{V} is about 10^{-2}, which is rather robust in comparing with the case without the gravitational quantum effects.

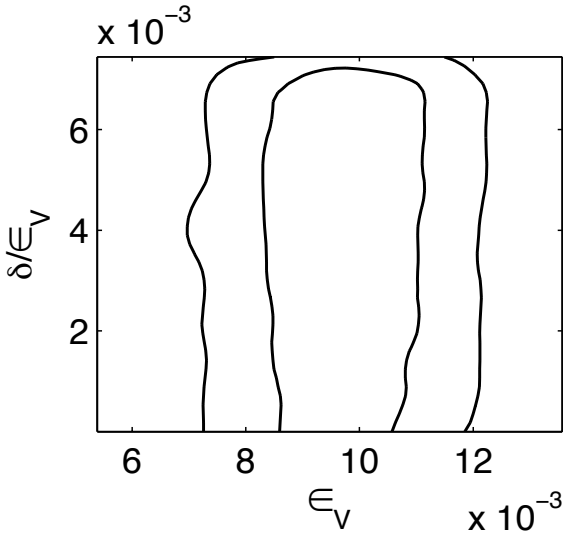

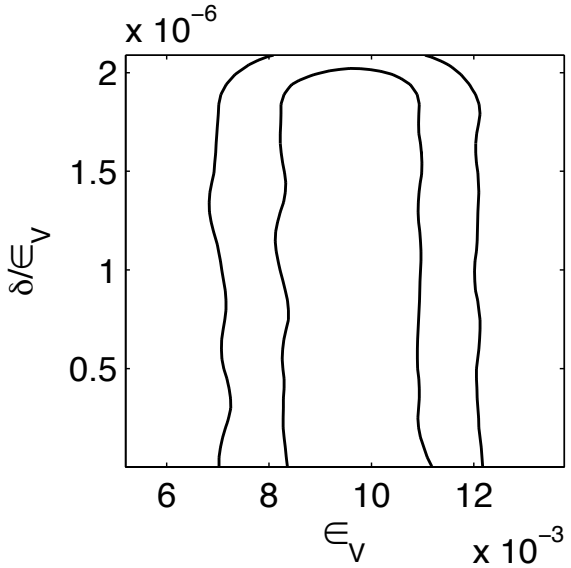

Table of Contents

Conclusions and future plan

- Quantum gravitational effects in the early universe are important and need to be taken into account with the arrival of the era of precision cosmology.
- The uniform approximation method is designed to study analytically the evolution of the mode functions of perturbations generated in the early universe with such effects.
- The analytical results of power spectra and spectral indices are explicitly obtained in general case to the first-order approximations with the error bounds $\lesssim 15\%$.

Conclusions and future plan (Cont.)

- To the third-order, the analytical results of power spectra and spectral indices are explicitly obtained in the case with only one-turning point with the error bounds $\lesssim 0.15\%$.
- Applying them to the k-inflation, we obtained the most accurate results for power spectra, spectral indices and runnings, existing so far in the literature.
- Applying them to LQC, we found that the quantum gravitational effects from inverse-volume corrections are within the detection of the next (Stage IV) experiments [20].

[20] K. N. Abazajian et al., arXiv:1309.5381.

Conclusions and future plan (Cont.)

- It would be very important to generalize our above studies to the cases with more than one turning point.
- Applying our method to study quantum gravitational effects for other models, including the ones from supergravity, strong/M-Theory and Horava-Lifshitz theory of quantum gravity.
- It is certainly desirable to find observational signals for future experiments/observations.
- …….

Acknowledgements

Work was supported in part by:

a) DOE Grant:
DE-FG02-10ER41692

b) NSFC Grant:
No. 11375153

c) Ciência Sem Fronteiras:
No. 004/2013 - DRI/CAPES

Thank You!